Technical Note

Metamorphosing the SASW Method by 2D Wavefield Transformation

Chun-Hung Lin[1] and Chih-Ping Lin[2]

Abstract: Dispersion analysis in surface wave testing is conventionally associated with a certain method of data acquisition, such as phase angle analysis in the two-station spectral analysis of surface wave (SASW) method and two-dimensional (2D) multistation wavefield transformation in the multistation analysis of surface wave (MASW) method. A new procedure has been developed to reconstruct the SASW data as MASW-imitating data, taking advantage of the 2D multistation wavefield transformation to better analyze the SASW data. Numerical simulations and a real-world example demonstrate the feasibility of this procedure, but also reveal an unwanted side effect associated with aliasing. A common-receiver survey is proposed for future experiments to eliminate this unwanted side effect and at the same time increase the lateral resolution. **DOI: 10.1061/(ASCE)GT.1943-5606.0000657.** © *2012 American Society of Civil Engineers.*

CE Database subject headings: Shear waves; Surface waves; Data collection; Simulation; Transformations.

Author keywords: Shear waves; Surface waves; SASW; MASW; Wavefield transformation.

Introduction

The surface wave method has gained popularity in engineering practice for determining S-wave velocity (V_s) depth profiles. The main advantage of the method is essentially related to its nondestructive and noninvasive nature that allows characterization of hard-to-sample soils without the need for boreholes that make the subsurface seismic methods (such as downhole and cross-hole methods) expensive and time-consuming.

Three steps are involved in a surface wave test: (1) field testing for recording surface waves, (2) determination of the experimental dispersion curve from the field data, and (3) inversion of the V_s profile from the experimental dispersion curve. Different surface wave methods are often referred to based on how the seismic data are acquired and how the dispersion curve is analyzed from the data. At present, two-station spectral analysis of surface wave (SASW) and multistation analysis of surface wave (MASW) are the most popular methods used worldwide. The two-station SASW method is based on the phase difference between two receivers as a function of frequency (Nazarian and Stokoe 1984), whereas the multistation MASW method is based on the relation between phase angles and the source-to-receiver offset (Lin and Chang 2004), or 2D wavefield transformation of surface wave (e.g., McMechan and Yedlin 1981; Gabriels et al. 1987; Park et al. 1998; Xia et al. 2007).

Limited to two-channel data, the conventional dispersion analysis of SASW suffers from possible phase unwrapping errors, inefficient data filtering for near and far field effects and synthesis of dispersion curves from different offsets, and inability to distinguish multiple modes (Lin and Chang 2004). MASW, on the other hand, can overcome these problems and provide visualization of the dispersion relation through 2D wavefield transformation. Although the number of channels in a seismograph may restrict the field-testing procedure, it does not necessarily prescribe the method of dispersion analysis. This paper proposes a procedure to reconstruct the SASW data as MASW-imitating data so that a relaxed 2D wavefield transformation can be applied. The proof of concept is first given by numerical simulations, followed by a real-world example. An unwanted side effect of the new procedure is discussed and a countermeasure is proposed, leading to a better experimental configuration with higher lateral resolution.

Two-Dimensional Wavefield Transformation of SASW data

In the following, a new procedure for analyzing SASW data is introduced to take advantage of the multistation approach. This procedure involves reconstruction of the SASW data and relaxation of the 2D wavefield transformation.

Source-to-Receiver Distance Gather

The source-to-receiver distance gather has been used to combine sets of seismic records from different shotpoints, thereby simulating long-range data when the number of recording channels is not large enough (Gabriels et al. 1987; Ryden et al. 2002). To apply wavefield transformation on SASW data, we proposed a preprocess to rearrange and reconstruct the SASW data by source-to-receiver distance gather to generate MASW-imitating data, followed by a relaxed 2D wavefield transformation. Each pair of signals from different shots in an SASW testing was identified by the source-to-receiver distance. The SASW data were then rearranged in ascending order of source-to-receiver distance. Between two adjacent shots, signals having the same source-to-receiver distance can be simply stacked and averaged. When there is strong lateral variation within the testing area or when source-related errors are significant, signals with the same source-to-receiver distance may not be identical, resulting in a phase difference between the signals with the same source-to-receiver offset. At each frequency, this static phase error between the last waveform of the preceding shot and the first waveform of the subsequent shot can be determined and then

[1]Ph.D. Candidate, National Chiao Tung Univ., Hsinchu, 300, Taiwan.
[2]Professor, National Chiao Tung Univ., Hsinchu, 300, Taiwan (corresponding author). E-mail: cplin@mail.nctu.edu.tw

Note. This manuscript was submitted on October 1, 2010; approved on November 1, 2011; published online on November 3, 2011. Discussion period open until January 1, 2013; separate discussions must be submitted for individual papers. This technical note is part of the ***Journal of Geotechnical and Geoenvironmental Engineering***, Vol. 138, No. 8, August 1, 2012. ©ASCE, ISSN 1090-0241/2012/8-1027–1032/$25.00.

J. Geotech. Geoenviron. Eng. 2012.138:1027-1032.

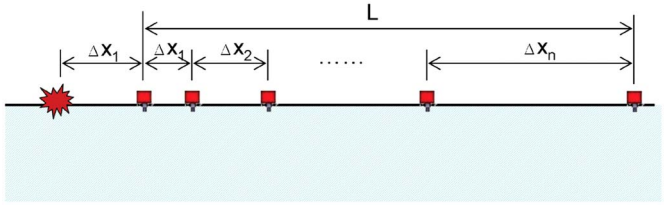

Fig. 1. Source-to-receiver distance gather of SASW data

Table 1. Parameters of Earth Models Used in Numerical Simulations

Model	Layer	V_s(m/s)	V_p(m/s)	Layer thickness (m)	Density (g/ cm^3)
1	1	300	600	10	1.8
	2	400	800	∞	1.8
2	1	300	600	4	1.8
	2	250	500	8	1.8
	3	400	800	∞	1.8

deducted from all traces of the subsequent shots. This data reduction procedure is referred to as the "phase-seaming procedure" in Lin and Lin (2007). After "seaming" all adjacent shots, the reconstructed data mimics MASW data, as shown in Fig. 1. The major difference between MASW data and MASW-imitating data is that MASW signals are normally equally spaced, whereas MASW-imitating signals from SASW data are not. The wavefield transformation can be modified to accommodate spatially nonuniform data, as will be shown.

Spatially Nonuniform Wavefield Transformation

Similar to an ordinary, uniform 2D multistation wavefield transformation, the dispersion analysis begins with a Fourier transform with respect to time. This can be done by a discrete Fourier transform (DFT) using the Fast-Fourier transform (FFT) algorithm, in which the frequency domain is uniformly discretized to obtain the discretized wavefield in the frequency-space domain $U(f_i, x_n)$

$$U(f_i, x_n) = \frac{1}{M}\sum_{m=0}^{M-1} u(t_m, x_n)\exp(-j2\pi f_i t_m) \tag{1}$$

where u = ground motion (typically velocity) sampled by the receivers with time interval Δt and number of points M, $j = \sqrt{-1}$, $t_m = m\Delta t, f_i = i\Delta f = i/[(M-1)\Delta t]$, and x_n = location of the receiver. The subscripts n, m, and i in Eq. (1) are integer indices to represent, respectively, discrete points in the space, time, and frequency domains. For conventional MASW data, another FFT with respect to space can be performed to obtain the frequency-wavenumber $(f-k)$ spectrum. However, this is not possible with the MASW-imitating data from SASW testing because it is not uniform in the space domain. The form of the discrete-space Fourier transform is relaxed to accommodate nonuniform data in the space domain, as

$$Y(f_i, k) = \sum_{n=0}^{N-1} U(f_i, x_n)\exp(-j2\pi k x_n) \tag{2}$$

where the $f-k$ spectrum $Y(f_i, k)$ represents the discrete-frequency wavefield in the frequency-wavenumber domain. Eq. (2) takes the form of a discrete-space Fourier transform, but it is not a rigorous Fourier transform in that x_n is nonuniformly spaced. It is, in essence, equivalent to the frequency domain beamformer (Zywicki 1999), which deals with general multidimensional spatial array problems. The wavenumbers of the propagating modes for each frequency can be identified at amplitude peaks of the spectrum $Y(k)$. The corresponding phase velocity is then determined by the definition $v = 2\pi f/k$. Alternatively, the $f-v$ spectrum can be derived by substituting $k = 2\pi f/v$ into Eq. (2).

Numerical Verification

To demonstrate the feasibility and advantages of the proposed method, the proof of concept is first given by two numerical examples followed by a field example. In the numerical verification, two distinct earth models were selected; one is a normal profile with a dominant fundamental mode and the other is a reversal profile with multiple dominant modes. The parameters of the earth models used are listed in Table 1. Both SASW and MASW testing were numerically simulated. The common-midpoint receiver spacings for the SASW testing included 2, 4, 8, 16, 32, and 64 m. The receiver spacing for the ordinary MASW testing was 2 m. Synthetic waveforms for the surface wave testing were simulated by the modal summation method programmed by Herrmann and Ammon (2002).

Model 1 was a simple two-layer model with a lower-velocity top layer ($V_s = 300$ m/s) overlying a higher-velocity half-space ($V_s = 400$ m/s). Fig. 2(a) shows the result of the proposed dispersion analysis using 2D wavefield transformation on the six-shot SASW data in Model 1. Also shown in Fig. 2 for comparisons are the experimental dispersion curves obtained from the conventional SASW analysis [Fig. 2(b)] and the ordinary, equally spaced MASW [Fig. 2(c) for short geophone spread, $L = 24$ m, and Fig. 2(d) for long geophone spread, $L = 128$ m]. The spread length of the long MASW was selected to be equal to the maximum source-to-receiver offset in the SASW testing for direct comparison. In the normal dispersive case, where the fundamental mode dominates throughout the frequency range of interest, the dispersion curves obtained from different receiver spacings in the SASW testing are consistent. Both the conventional SASW dispersion analysis [Fig. 2(b)] and the new proposed method [Fig. 2(a)] obtain a fundamental-mode dispersion curve identical to the analytical solution; not surprisingly, so does the ordinary MASW testing [Fig. 2(c) or Fig. 2(d)]. Compared with the uniform wavefield transformation from the ordinary MASW testing [Figs. 2(c) and 2(d)], the nonuniform wavefield transformation from the SASW testing [Fig. 2(a)] shows some aliasing patterns in the 2D spectrum attributable to sparse sampling in the space domain. Nevertheless, the correct dispersion curve can be clearly distinguished from the aliasing pattern in the $f-v$ domain.

The Model 2 earth profile comprised two layers over a half-space ($V_s = 400$ m/s). The first layer was 4 m thick and 300 m/s in V_s. The second layer was the low-velocity layer, 8 m thick and 250 m/s in V_s. The corresponding dispersion analyses for Model 2 are shown in Fig. 3. Fig. 3(a) shows that the proposed dispersion analysis reveals different modes of dispersion curves, agreeing well with the results from the wavefield transformation analysis of the long MASW analysis in Fig. 3(d). Although there are some aliasing effects caused by nonuniform spatial sampling, particularly in the left part of the spectral image [Fig. 3(a)], dominant modes can still be recognized successfully. In contrast,

J. Geotech. Geoenviron. Eng. 2012.138:1027-1032.

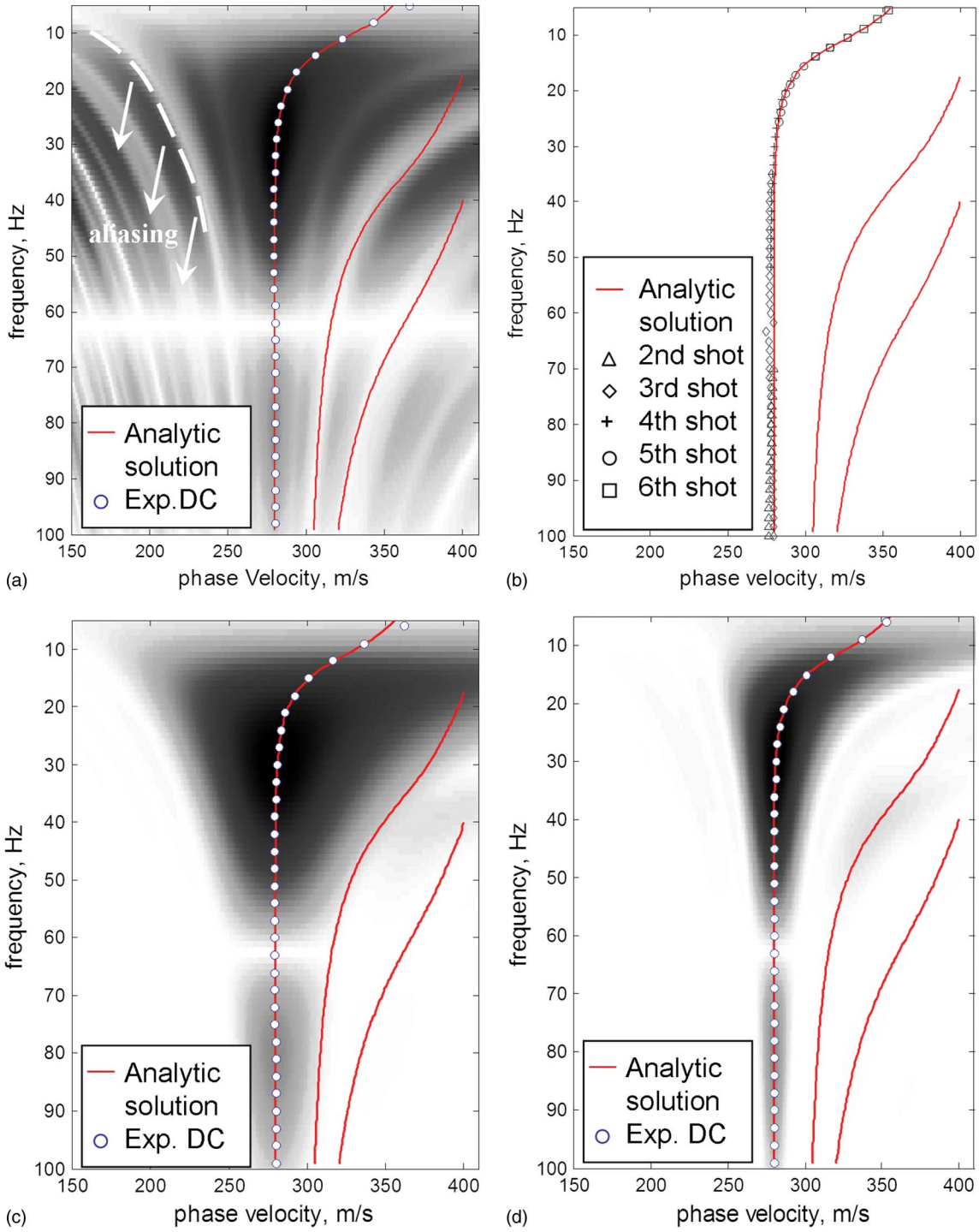

Fig. 2. Dispersion analyses for Model 1: (a) nonuniform wavefield transformation analysis on six-shot SASW data, with circles showing the experimental dispersion curve (Exp. DC); (b) dispersion curves from conventional SASW analysis; (c) uniform wavefield transformation analysis on MASW data, $\Delta x = 2$ m, $L = 24$ m; (d) uniform wavefield transformation analysis on MASW data, $\Delta x = 2$ m, $L = 128$ m

the experimental dispersion curves extracted from the conventional SASW analysis [Fig. 3(b)] gradually sway from one mode to another. There is no apparent inconsistency between the adjacent receiver spacings. It is difficult to tell whether higher modes dominate at certain frequency ranges. The experimental dispersion curves obtained from the conventional SASW analysis [Fig. 3(b)] are similar to the results of the short MASW analysis [Fig. 3(c)]. The 2D wavefield transformation is unable to separate modes if the geophone spread is not sufficiently long. However, even in the short MASW analysis, the 2D spectrum image does depict suspiciously higher dominant modes at higher frequencies. Therefore, the 2D wavefield transformation analysis on the SASW testing data is a good supplement to the conventional SASW analysis, if not to replace it. It provides a quick visualization of the energy distribution in the $f - v$ domain to help identify possible higher dominant modes and validate the SASW analysis.

J. Geotech. Geoenviron. Eng. 2012.138:1027-1032.

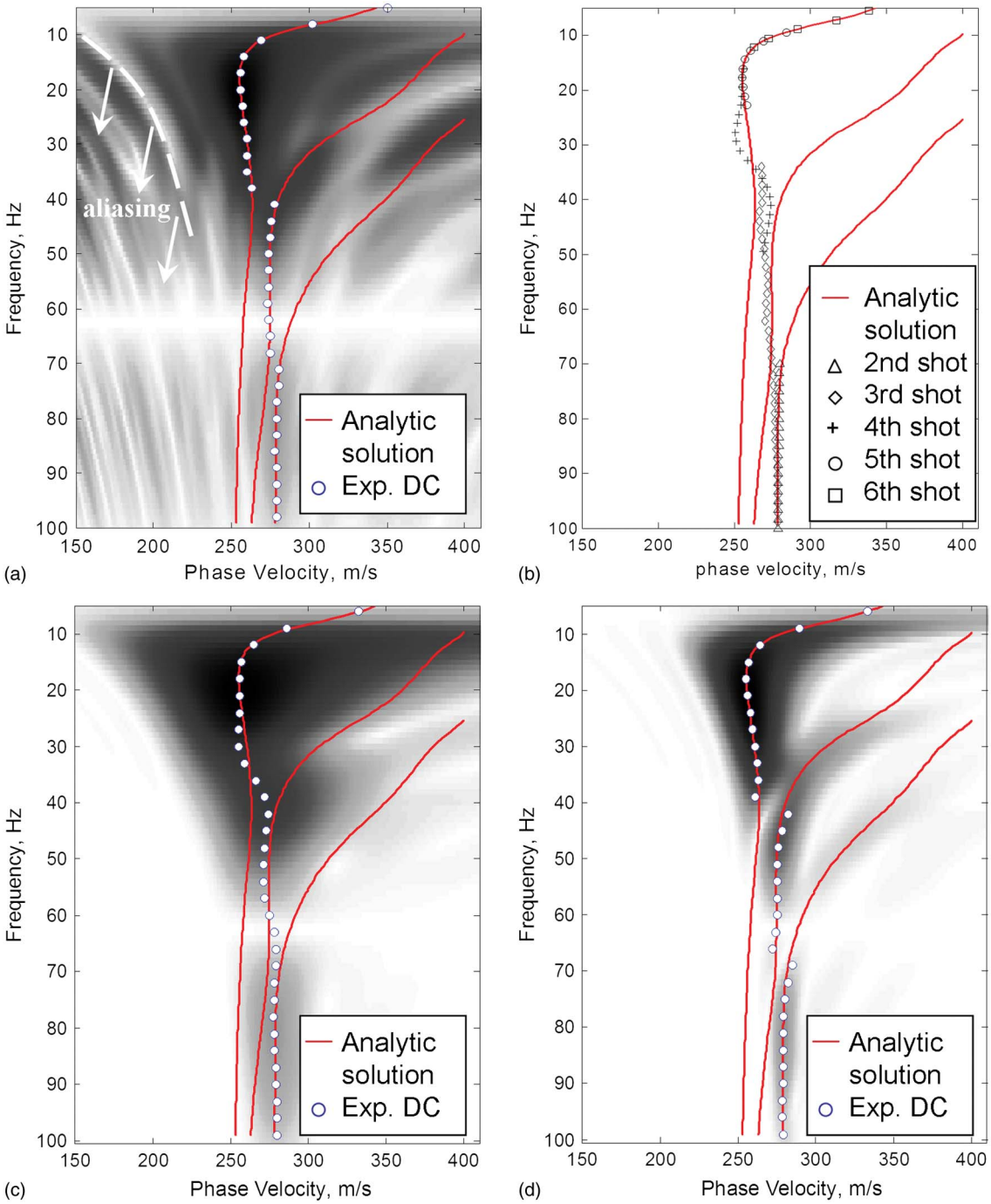

Fig. 3. Dispersion analyses for Model 2: (a) nonuniform wavefield transformation analysis on six-shot SASW data, with circles showing the experimental dispersion curve (Exp. DC); (b) dispersion curves from conventional SASW analysis; (c) uniform wavefield transformation analysis on MASW data, $\Delta x = 2$ m, $L = 24$ m; (d) uniform wavefield transformation analysis on MASW data, $\Delta x = 2$ m, $L = 128$ m

Field Example

A field example was demonstrated at a test site next to the Luodong Sports Park in Luodong Township, Taiwan. The test site is mainly composed of silty sand within the top 20 m. A power transformer substation is to be constructed at this site. Previous site investigation revealed possible liquefaction during large earthquakes based on standard penetration tests (SPTs) and suggested ground improvement by jet grouting. Surface wave tests were conducted prior to jet grouting to serve as the baseline for assessment of ground improvement based on V_s. Both common-midpoint SASW (CMP-SASW) and MASW signals were acquired with 4.5-Hz vertical geophones and a 62.5-μs sampling interval. A sledgehammer impacting on a steel plate was used as the seismic source. Four shots were conducted for the CMP-SASW with receivers spaced at 2, 4, 8, and 16 m, respectively, which could be reorganized into 32-m-long MASW-imitating data. For comparison, a 32-m-long MASW test with 2-m receiver spacing and 2-m near offset was also conducted. The midpoint of the MASW survey line coincided with that of the CMP-SASW survey line, so the two tests had similar sampling ranges in space.

J. Geotech. Geoenviron. Eng. 2012.138:1027-1032.

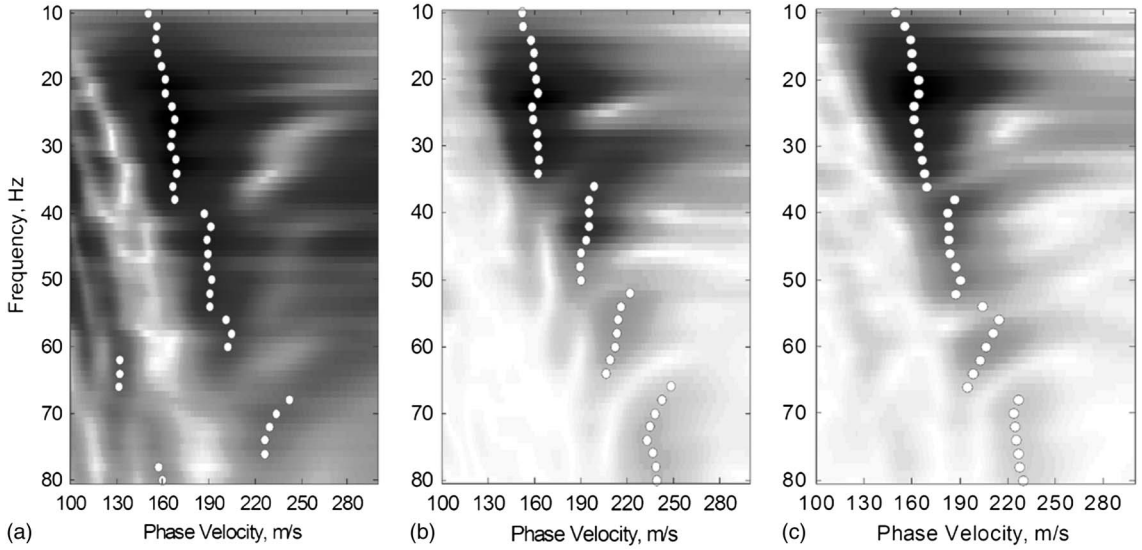

Fig. 4. Results of dispersion analyses in the field example: (a) nonuniform wavefield transformation analysis on four-shot SASW data; (b) uniform wavefield transformation analysis on MASW data, with the same midpoint and spread length as the SASW test; (c) uniform wavefield transformation analysis on a 16-shot common two-receiver configuration survey

The results of nonuniform wavefield transformation using SASW data and uniform wavefield transformation using MASW data are shown in Figs. 4(a) and 4(b), respectively. The nonuniform wavefield transformation analysis on the SASW data reveals multiple modes and yields dispersion data similar to the conventional MASW. The points of the experimental dispersion curves in these two figures were picked at the absolute peaks in the spectra. The differences around 65 and 80 Hz are because of false energy peaks from aliasing, as is also demonstrated in the numerical simulations. These erroneous data points can be readily corrected by screening out the aliasing zone when searching for energy peaks in the spectrum.

Common-Receiver Configuration

As shown in both the numerical and real-world examples, the wavefield transformation analysis on SASW data had poorer resolution and was contaminated by aliasing effects attributable to a smaller number of sampling points and nonuniform receiver spacing. Therefore, instead of a common-midpoint configuration conventionally adopted in a SASW test, a common-receiver configuration is proposed to eliminate this unwanted effect. A generic common-receiver configuration is shown in Fig. 5, in which the geophone spread is fixed and the data of different source-to-receiver distances are collected by gradually increasing the near offset in multiples of receiver spacing. More-equally spaced data can be recorded by these walk-away shots, which allows assembling uniform MASW-imitating data by the source-to-receiver gather.

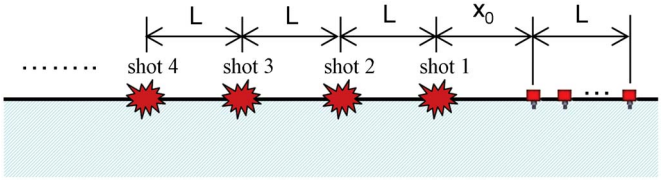

Fig. 5. The generic common-receiver configuration

This idea was tested in the Luodong test site. Two receivers 2 m apart were placed at the same midpoint as in the first step of the conventional SASW testing. Sixteen walk-away shots were conducted to assemble a 32-m-long, MASW-imitating dataset to have the same spread length as the previous four-shot CMP-SASW and conventional MASW array. The result of the dispersion analysis is shown in Fig. 4(c). Compared with Fig. 4(a), the aliasing effect is eliminated and both the spectral image and the extracted dispersion curve are almost identical to Fig. 4(b) for the conventional MASW.

When there are only two geophones or two recording channels available, a common-receiver configuration is a better way to acquire surface wave data for wavefield transformation analysis. Furthermore, the common-receiver configuration not only avoids the aliasing problem, it also increases the lateral resolution in spatial sampling by fixing the short geophone spread in the same location (Lin and Lin 2007). In this extreme example, the geophone spread was as small as 2 m, which is even smaller than the smallest wavelength recordable. In practice, the number of shots can be greatly reduced by longer geophone spread when more receivers and recording channels are available, as shown in Lin and Lin (2007). For example, with four receivers in 2-m intervals, the example experiment can be accomplished by six walk-away shots on the 6-m receiver spread.

Conclusions

Limited to two-channel data, conventional dispersion analysis of SASW suffers from possible phase unwrapping errors, inefficient data filtering and synthesis, and inability to distinguish multiple modes. MASW, on the other hand, can overcome these problems and provide visualization of the dispersion relation through multistation 2D wavefield transformation. A new procedure is proposed to reconstruct the SASW data as MASW-imitating data by the source-to-receiver distance gather and analyze the data by the relaxed 2D wavefield transformation, taking advantage of the multistation approach in processing SASW data. Numerical simulations

J. Geotech. Geoenviron. Eng. 2012.138:1027-1032.

and a field example demonstrate the feasibility of this new approach and support the idea that the method of dispersion analysis is not restricted by the number of recording channels. However, the numerical simulations and a field example also revealed poorer resolution and aliasing patterns for common-midpoint SASW resulting from nonuniform receiver spacing in the MASW-imitating data. To eliminate this unwanted side effect and increase the lateral resolution at the same time, for future experiments a common-receiver configuration in conjunction with walk-away shots is recommended over the common-midpoint configuration conventionally adopted in the SASW method.

References

Gabriels, P., Snieder, R., and Nolet, G. (1987). "In situ measurements of shear-wave velocity in sediments with higher-mode Rayleigh waves." *Geophys. Prospect.*, 35(2), 187–196.

Herrmann, R. B., and Ammon, C. J. (2002). *Computer programs in seismology*, Version 3.20, St. Louis University, St. Louis, MO.

Lin, C.-P., and Chang, T.-S. (2004). "Multi-station analysis of surface wave dispersion." *Soil Dyn. Earthquake Eng.*, 24(11), 877–886.

Lin, C.-P., and Lin, C.-H. (2007). "Effect of lateral heterogeneity on surface wave testing: numerical simulations and a countermeasure." *Soil Dyn. Earthquake Eng.*, 27(6), 541–552.

McMechan, G. A., and Yedlin, M. J. (1981). "Analysis of dispersive waves by wave-field transformation." *Geophysics*, 46(6), 869–874.

Nazarian, S., and Stokoe, K. H., II. (1984). "Nondestructive testing of pavements using surface waves." *Transportation Research Record 993*, Transportation Research Board, Washington, DC, 67–79.

Park, C. B., Miller, R. D., and Xia, J. (1998). "Imaging dispersion curves of surface waves on multi-channel record." *Proc., 68th Annual Int. Meeting, Society of Exploration Geophysicists*, Expanded Abstracts, Society of Exploration Geophysicists, Tulsa, OK, 1377–1380.

Ryden, N., Ulriksen, P., Ekdahl, U., Park, C. B., and Miller, R. D. (2002). "Portable seismic acquisition system for pavement MASW." *Proc., Symp. on the Application of Geophysics to Engineering and Environmental Problems (SAGEEP 2002)*, Engineering Geophysical Society, Denver, CO, February 10-14, 2002.

Xia, J., Xu, Y., and Miller, R. D. (2007). "Generating image of dispersive energy by frequency decomposition and slant stacking." *Pure Appl. Geophys.*, 164(5), 941–956.

Zywicki, D. J. (1999). "Advanced signal processing methods applied to engineering analysis of seismic surface wave." Doctoral dissertation, Dept. of Civil Engineering, Georgia Institute of Technology, Atlanta, GA.

J. Geotech. Geoenviron. Eng. 2012.138:1027-1032.